



# Exogenous interleukin-1 $\alpha$ signaling negatively impacts acquired chemoresistance and alters cell adhesion molecule expression pattern in colorectal carcinoma cells HCT116

Pranas Grigaitis<sup>a,1</sup>, Violeta Jonusiene<sup>a</sup>, Vilmante Zitkute<sup>a</sup>, Justas Dapkunas<sup>b</sup>,  
Daiva Dabkevičienė<sup>a,\*</sup>, Ausra Sasnauskienė<sup>a</sup>

<sup>a</sup> Institute of Biosciences, Life Sciences Center, Vilnius University, Sauletekio al. 7, Vilnius 10227, Lithuania

<sup>b</sup> Institute of Biotechnology, Life Sciences Center, Vilnius University, Sauletekio al. 7, Vilnius 10227, Lithuania

## ARTICLE INFO

### Keywords:

Acquired chemoresistance  
Colorectal cancer  
Interleukin-1 $\alpha$   
Cell death  
Cell adhesion

## ABSTRACT

Proinflammatory cytokine and chemokine signaling from the tumor microenvironment is thought to be crucial for developing and sustaining colorectal cancer by regulating a multitude of pathways associated with a variety of cellular mechanisms. Among these pathways there is acquired chemoresistance, which is usually a major obstacle in the way towards successful chemotherapeutic treatment of advanced colorectal cancer cases. Despite of an emerging body of data published on the role of cytokine signaling network in cancer, little is known about the effects of the upstream cytokine interleukin-1 $\alpha$  (IL-1 $\alpha$ ) signaling to the cancer cells. In this study we have shown that the increase in exogenous IL-1 $\alpha$  signaling increases chemosensitivity of both chemosensitive and chemoresistant colorectal cancer cell lines, treated with a widely used cytotoxic antimetabolite 5-fluorouracil (5-FU). This was a result of increased cell death but not of the changes in 5-FU-induced cell cycle arrest. Noticeably, combined exogenous IL-1 $\alpha$  and 5-FU treatment had significant effects on the expression of cell adhesion molecules, suggesting a decrease in adhesion-dependent chemoresistance and, on the other hand, an increase in metastatic potential of the cells. These results lead to a conclusion that modulation of IL-1 receptor activity could have applications as a part of combination therapy for advanced and highly metastatic colorectal cancers.

## 1. Introduction

Colorectal cancer (CRC) is one of the most prevalent oncological diseases, reported to be the second most common type of cancer globally [1]. The standard routine of treatment for stage I-III CRC cases is the removal of the primary tumor. For stage III-IV cancers it is followed by combined chemotherapeutic treatment which usually includes 5-fluorouracil (5-FU) as the major component [2]. However, one of the major challenges in treatment of patients with advanced CRC is the acquisition of chemoresistance that limits the success of the treatment and decreases the rate of patient survival.

There is a body of evidence that tumors are vastly dependent on the inflammation-associated processes, namely, the proinflammatory

microenvironment that is formed at the sites of primary tumors. This microenvironment is highly shaped by tumor cells themselves, together with major contributions by both non-malignant and recruited immune cells, as well as their secretome. Therefore, the extensive chemical signaling between cancer cells and proinflammatory tumor microenvironment via chemokines and cytokines is thought to regulate many aspects of cancer cells, such as their proliferation, cell death, migration and invasion [3], as well as response to targeted therapy (e.g., EGFR inhibition; [4]). It is believed that one of the major contributors mediating the signal transduction between tumor microenvironment and cancer cells is interleukin-1 $\alpha$  (IL-1 $\alpha$ ), a proinflammatory upstream cytokine which binds interleukin-1 receptor (IL-1R) to induce the intracellular response. Besides binding to the cell surface receptor, IL-1 $\alpha$

*Abbreviations:* CRC, colorectal cancer; IL, interleukin; ECM, extracellular matrix; 5-FU, 5-fluorouracil; OxaPt, oxaliplatin; rh, recombinant human [protein]; Md, median; IQR, interquartile range; PPI, protein-protein interaction; dsDNA, double-stranded DNA

\* Corresponding author.

*E-mail addresses:* [pranas.grigaitis@bioquant.uni-heidelberg.de](mailto:pranas.grigaitis@bioquant.uni-heidelberg.de) (P. Grigaitis), [violeta.jonusiene@gf.vu.lt](mailto:violeta.jonusiene@gf.vu.lt) (V. Jonusiene), [vilmante.zitkute@gf.vu.lt](mailto:vilmante.zitkute@gf.vu.lt) (V. Zitkute), [justas.dapkunas@bti.vu.lt](mailto:justas.dapkunas@bti.vu.lt) (J. Dapkunas), [daiva.dabkevičienė@gf.vu.lt](mailto:daiva.dabkevičienė@gf.vu.lt) (D. Dabkevičienė), [ausra.sadauskaite@gf.vu.lt](mailto:ausra.sadauskaite@gf.vu.lt) (A. Sasnauskienė).

<sup>1</sup> Present address: Center for Quantitative Analysis of Molecular and Cellular Biosystems (BioQuant), Heidelberg University, Im Neuenheimer Feld 267, Heidelberg 69120, Germany.

<https://doi.org/10.1016/j.cyto.2018.11.031>

Received 17 August 2018; Received in revised form 19 November 2018; Accepted 25 November 2018

Available online 22 December 2018

1043-4666/ © 2018 Elsevier Ltd. All rights reserved.

also possesses a nuclear localization sequence, because of which it might be transported to the nucleus and bind to chromatin. Thus, IL-1 $\alpha$  is considered to be a dual-function cytokine [5], however, the functions of nuclear IL-1 $\alpha$  are still far from being fully understood.

Even though the role of immune signaling pathways in cancerogenesis is widely studied, little is known about contribution of IL-1 $\alpha$  to the proinflammatory tumor microenvironment, disease progression and, specifically, chemoresistance of cancer cells. In abstract terms, among other proinflammatory cytokines IL-1 $\alpha$  is thought to control the pathways contributing to stress response, cell migration and differentiation [6]. Aiming to elucidate the role of IL-1 $\alpha$  signaling in acquired chemoresistance, in this study we investigated the connection between exogenous IL-1 $\alpha$  signaling and colorectal cancer cell response to 5-FU-induced cytotoxic stress, using both chemosensitive and chemoresistant CRC cell models and comparing the effects between them.

First, we treated parental chemosensitive HCT116 cells with recombinant human IL-1 $\alpha$  and assessed mRNA expression of selected cytokines and their receptors. The results of mRNA expression assays were used to construct a protein-protein interaction network, which was functionally annotated to identify the pathways and cellular properties that could be altered due to modulation of IL-1 receptor activity. In order to validate these predictions, we investigated the effect of exogenous IL-1 $\alpha$  signaling to both parental colorectal cancer cells HCT116 and their 5-FU-resistant subline HCT116/FU. We have shown that, after combined treatment of cells with exogenous IL-1 $\alpha$  and 5-FU, the increase of chemosensitivity of both cell lines is due to increase in either necrotic or both necrotic and apoptotic cell death, and we did not detect any effects of combination treatment on 5-FU cytotoxicity-induced cell cycle arrest. In addition, we observed alterations in cell morphology upon treatment with exogenous IL-1 $\alpha$ . Consequently, we determined changes in mRNA expression of a number of cell adhesion molecules upon either IL-1 $\alpha$  treatment or its combination with 5-FU cytotoxic treatment.

## 2. Materials and methods

### 2.1. Cell lines

CRC cells HCT116 (MSI, TP53 proficient, K-Ras-mutated) were purchased from the ATCC. HCT116/FU subline was generated in our laboratory by continuous cultivation of HCT116 cells in medium containing 5-fluorouracil for 1 year until acquisition of stable resistance, i.e., achieving the half-inhibitory concentration (IC<sub>50</sub>) under 10 times higher 5-FU concentrations than in case of the parental cell line [7]. Both cell lines were cultured in RPMI 1640 medium (Biochrom GmbH), supplemented with 10% fetal bovine serum, 2 mM L-glutamine and 0.05 mg/mL gentamicin in a humidified atmosphere at 37 °C in 5% CO<sub>2</sub>.

### 2.2. Cell treatment protocol

Cell treatment schedule is shown in Fig. 1. Recombinant human interleukin-1 $\alpha$  and interleukin-1 receptor antagonist (rhIL-1 $\alpha$  and rhIL-1Ra, respectively; R&D Systems) were added to culture medium at appropriate concentrations right after seeding of the cells. 2.5 ng of recombinant protein per milliliter of cultivation medium was used, if not specified otherwise. rhIL-1Ra was used as a negative control for rhIL-1 $\alpha$  effect verification. Cytotoxic agents 5-fluorouracil (5-FU, 50 mg/mL, Accord Healthcare) and oxaliplatin (OxaPt, 5 mg/mL, Accord Healthcare) were used for experiments. The drugs were diluted in cell culture medium to final concentrations of: 0.1 mM 5-FU for HCT116 cells, 1 mM 5-FU for HCT116/FU cells or 0.05 mM OxaPt for both cell lines.

### 2.3. Cell viability assay by crystal violet

Cells were once rinsed with PBS and fixed in 96% ethanol for 10 min, then 0.05% crystal violet solution in 20% ethanol was added for 30 min, the cells were rinsed and the remaining dye was dissolved in 0.1% acetic acid solution in 50% ethanol. The absorbance at 585 nm was registered using microplate reader ASYS340 (Biochrom Ltd.).

### 2.4. RNA interference of *IL1A*

A small interfering (si)RNA, specific to human *IL1A* mRNA, si*IL1A* (5'-CAUCCAAGCUUACCUUCAAdTdT-3') and a non-targeting (having no significant homology to any human mRNA) siNT (5'-AGGUAGUGUAAUCGCCUUGdTdT-3') were purchased from MWG Biotech AG. Cells were seeded in culture medium without gentamicin and after 24 h were transfected with siRNA using Lipofectamine RNAiMAX (Invitrogen), according to the manufacturer's protocol. At 6 h after transfection, the cells were washed with PBS once, fresh culture medium with antibiotics was added, and after additional 18 h, cytotoxic treatment was performed as described before. The effectivity of transfection was assessed by qPCR using RNA extracted from cells (see below), collected 24 h after the addition of transfection mixture. Transfection with si*IL1A* yielded 3.11  $\pm$  0.21-fold less of *IL1A* transcript in the transfected cells, in comparison with transfection with non-targeting siRNA.

### 2.5. Flow cytometric analysis of cell cycle and induction of apoptotic cell death

Cellular DNA content was investigated using dsDNA-intercalating dye propidium iodide (PI). Cells were rinsed with PBS once, detached from the culture dish, 1  $\times$  10<sup>6</sup> cells were pelleted and fixed in 70% ethanol at +4 °C overnight. Fixed cells were washed in PBS and then resuspended in 0.5 mL PI/RNase Staining Buffer (BD Biosciences) for 15 min in room temperature. The relative cellular DNA content

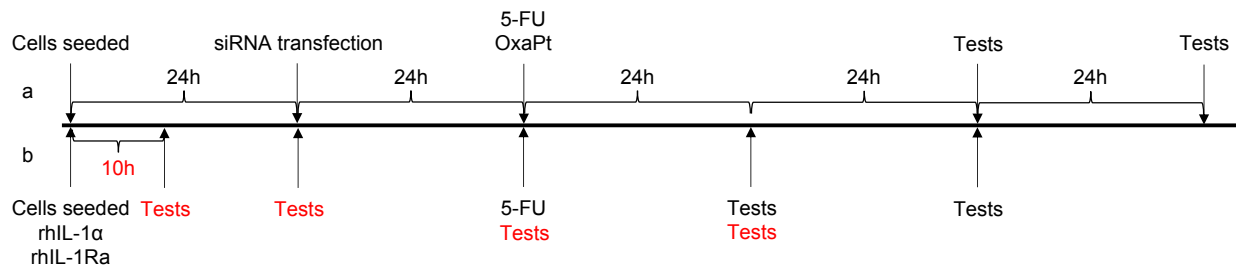


**Fig. 1.** Schedule of treatment. a. For *IL1A* silencing experiments, cells were transfected 24 h after seeding and treated with cytotoxic drugs 24 h after transfection, followed by tests 48 h after. b. For assays of impact of IL-1R ligands on cell viability, cell cycle and cell death mode analysis, as well as gene expression analysis, cell culture medium was supplemented with recombinant IL-1 $\alpha$  or IL-1Ra immediately after seeding, and cells were treated with 5-FU 48 h after seeding. Cells were collected for tests 24 or 48 h after treatment. For the time-course experiments of cytokine gene expression, cells were collected at 10, 24, 48 and 72 h after seeding (notations in red). (For interpretation of the references to color in this figure legend, the reader is referred to the web version of this article.)

(proportional to fluorescence of PI) was measured using flow cytometer FACSCalibur (BD Biosciences) and the data obtained was analyzed using CellQuest Pro software. Position in cell cycle ( $G_1$ , S and  $G_2$  cell cycle phases) and sub- $G_1$  (undergoing fragmentation of DNA, one of hallmarks of apoptotic cell death; [8]) cell subpopulations were assigned according to the relative PI fluorescence readout.

## 2.6. Cell death mode analysis by fluorescence microscopy

Cell death investigation was performed using double-stranded DNA-intercalating dyes acridine orange (AO) and propidium iodide (PI). Cells were detached from culture dish and collected together with cell incubation medium, pelleted and resuspended in PBS, supplemented with AO and PI (5  $\mu\text{g}/\text{mL}$  each). The microscopy was performed using epi-fluorescence microscope Olympus AX70, equipped with 60 $\times$  oil immersion objective (NA 1.25) and MF filter cube ( $\lambda_{\text{ex}}$  = 480–500 nm, 550–580 nm;  $\lambda_{\text{em}}$  = 515–535 nm, 590–625 nm). Cell counting (green nuclei, alive cells; bright green nuclei, apoptotic morphology; red nuclei, necrotic morphology) was carried out by a blinded investigator.

## 2.7. Quantitative real-time PCR

Total RNA from cells was extracted using GeneJET RNA Purification Kit (Thermo Scientific) and cDNA from 2  $\mu\text{g}$  of sample RNA was synthesized using Maxima First Strand cDNA Synthesis Kit for RT-qPCR (Thermo Scientific) according to manufacturer's protocol. Quantitative PCR was performed using the StepOnePlus Real-time PCR system (Applied Biosystems). Expression levels of genes (Table 1) were determined using Maxima SYBR Green/ROX qPCR Master Mix (Thermo Scientific). The gene expression changes were calculated using the  $2^{-\Delta\Delta\text{CT}}$  method, having the threshold cycle values ( $C_T$ ) determined from two independent RNA samples, each performed in triplicate, and normalized to an endogenous control gene *HPRT*. The expression change was considered significant when twofold or higher increase or decrease of the transcript level was observed.

The expression levels of *IL1A*, *IL6*, *IL7*, *CXCL8*, *IL11*, *IL13*, *IL18*, *IL23A*, *IL32*, *VEGFA*, *KITLG*, *TGFB*, *CSF2*, *EGF*, *CCL2*, *CXCR3*, *CXCR4*, *CXCL1*, *IL1R1* and *EGFR* were determined using gene-specific TaqMan probe and primer sets (TaqMan primer-probe sets and TaqMan Gene Expression Master Mix were obtained from Life Technologies). *HPRT*, *B2M* and *TBP* genes were used as endogenous control. The expression change was considered significant when twofold or higher increase or decrease of the transcript level was observed.

## 2.8. Protein-protein interaction (PPI) network construction

Information on physical PPIs of the seed nodes of the PPI network was acquired from the curated PPI databases IntAct [9] and BioGRID [10]. Upon collection, PPI lists were filtered out from low-confidence

interactions according to the method of detection used. The resulting network was visualized using CytoScape [11], and the members of the PPI network were functionally annotated by assigning Gene Ontology terms (GO, [12,13]) to the proteins of interest. Enrichment of the network in certain GO terms (in comparison to the reference set of human proteins,  $n = 20,972$ ) was determined using the resources of PantherDB server [14] and was accepted as significant with a  $p < 0.05$ . This enrichment is defined as the ratio between the fraction of proteins annotated by a certain GO term in the network and the fraction of such proteins in the reference set of human proteins.

## 2.9. Statistical analysis

The data are presented as means  $\pm$  SD from at least two independent assays, each one at least in triplicate, with an exception for the data from viability experiments (Section 3.2), which are presented as Md (IQR) from four independent assays, each one in triplicate. Cohen's  $d$  [15] was used as a measure of the effect size for those experiments. SigmaPlot 12.5 (Systat Software, Inc.) was used for data analysis and visualization. Student's  $t$ -test was used to compare two groups. Multiple comparisons were performed by Holm-Šidák *post-hoc* tests, following either one-way or repeated measures two-way ANOVA. Significance was accepted with  $p < 0.05$  and the effect size was considered to be very large with  $d > 1.2$ .

## 3. Results

### 3.1. Construction of exogenous *IL-1 $\alpha$* -dependent protein-protein interaction network and its functional annotation

The study was started from the characterization of the response of human colorectal carcinoma HCT116 cells at mRNA level to the stimulation with exogenous *IL-1 $\alpha$* . In order to introduce *IL-1 $\alpha$*  into the cell culture, we used recombinant human *IL-1 $\alpha$*  (rh*IL-1 $\alpha$* ), which we will refer to as “exogenous” or “rh*IL-1 $\alpha$* ” interchangeably in the rest of the report.

We monitored temporal mRNA dynamics of four selected cytokine-coding genes, *IL1A*, *IL32*, *IL6*, *CXCL1*, as well as *IL-1* receptor-coding *IL1R1* upon stimulation of HCT116 cells with exogenous *IL-1 $\alpha$*  at time points, spanning from 10 to 72 h (Fig. S1). We observed rather modest yet steady increase of *IL1A* transcript amount, in comparison to the expression changes of the downstream cytokines *IL32* and *CXCL1* (Fig. S1a). The rapid increase of high magnitude at mRNA level, followed by a relatively steep decrease in a time-dependent fashion indeed points into *IL-1 $\alpha$* -induced transcription of cytokine genes. Noticeably, the extent of mRNA upregulation is diminished at late time points, potentially due to the negative feedback loops. Curiously, expression of *IL6*, which is usually considered to be one of the main cytokines downstream of *IL-1 $\alpha$*  [16], was generally not significantly altered, except for a time point

**Table 1**  
List of primers for genes of interest, used in the study. (5'  $\rightarrow$  3').

Gene	Forward	Reverse
<i>IL1A</i>	GCTGCTGAAGGAGATGCCTGA	CAGACCTACGCTGGTTTTC
<i>IL32</i>	AGAGCTGGAGGACGACTTCA	TCATAATAAGCCGCCACTGTC
<i>CXCL1</i>	TGCTGAACAGTGACAAATCCA	TTCTCCTAAGCGATGCTCAAA
<i>IL1R1</i>	TTGCGTGGTAAGAAATTCATCTT	CCATATAAGGGCACACAAGTCC
<i>IL6</i>	AGCCCTGAGAAAGGAGACAT	TTTCAGCCATCTTTGAAGG
<i>VEGFA</i>	AAATGTGAATGCAGACCAAGA	ACACGTCTGCGGATCTTGTA
<i>CDH1</i>	CGTCTGGGCAGAGTGAAT	TTTGAATCGGGTGTCCGAGGG
<i>CDH2</i>	TGTTTGACTATGAAGGCAGTGG	TCAGTCATCACCTCCACCAT
<i>CTNNB1</i>	GACGGAGGAAGGTCTGAGGA	CAAATACCTCAGGGGAACAGG
<i>CLDN2</i>	ACTGTCCATCGGAAGATGCT	ACGCTGAGGAAGTTCTCCAA
<i>SELE</i>	GGCAGTTCGGGAAAGATCA	GTGGAGCTTCACAGGTAGG
<i>ITGB6</i>	TCTCCTGCGTGAGACACAAA	CACAGTCCCGTTACTCC
<i>VCL</i>	CCAAACATGTCTCTATATCCTGG	GAAGTGTCTTCAGACAGGG

**Table 2**  
List of upregulated and downregulated genes after 96 h treatment of HCT116 cells with rhIL-1 $\alpha$ .

Upregulation	Downregulation
<i>IL1A</i>	<i>IL11</i>
<i>IL32</i>	<i>CXCR4</i>
<i>CSF2</i>	<i>IL18</i>
<i>CXCL8</i>	<i>KITLG</i>
<i>IL23A</i>	<i>IL1R1</i>
<i>CXCL1</i>	

of 48 h (Fig. S1b). Another observation which could be attributed to the feedback mechanisms, was a fairly small downregulation of *IL1R1* transcript levels at the end of the time-course, suggesting alternative mechanisms being engaged to terminate the chronic IL-1 $\alpha$  signal. Examples of those could be internalization of IL-1R, post-transcriptional or post-translational regulation of receptor levels and others.

As we registered the extent IL-1 $\alpha$  signal-dependent mRNA expression to be significantly reduced at the last time point we measured (72 h), we put a hypothesis ahead that a steady-state condition might be successfully acquired at the time point of 96 h. Thus, this kind of system would preserve most of the characteristics arising from prolonged IL-1 $\alpha$  signaling, at the same time revealing putative feedback mechanisms. Therefore, to further investigate the response of external IL-1 $\alpha$  stimulus on HCT116 cells, we quantified the changes in cytokine mRNA expression after 96 h, using TaqMan probes.

A significant increase in transcript amount of *IL1A*, *IL32*, *CSF2*, *CXCL8*, *IL23A* and *CXCL1* and a significant decrease in mRNA expression of *IL11*, *CXCR4*, *IL18*, *KITLG* and *IL1R1* was detected (Table 2, Fig. S2). In order to evaluate the interplay between cytokine signaling and the effector proteins, as well as to determine the downstream pathways which could be affected by increased IL-1R activation in the cells, we constructed a protein-protein interaction (PPI) network from the publicly available data of physical PPIs, using the products of transcripts from Table 2, along with the respective receptors of those cytokines, as seed nodes (Fig. 2). Gene Ontology (GO) terms were subsequently used to functionally annotate the members of the PPI network, by assigning relevant GO terms to each protein of the network. The enrichment of certain GO terms in our network, compared to the standard set of human proteins, was calculated as described in Section 2.

With regard to the reference human gene set, the GO term analysis has shown enrichment of a number of GO terms in our PPI network (Table 3). It suggests that several diverse cellular processes and pathways might be affected upon treatment of HCT116 cells with rhIL-1 $\alpha$ . We observed an enrichment in proteins that participate in pathways playing role in cell survival (e.g., JAK-STAT cascade, NF- $\kappa$ B signal cascade) and cell death (proteins of JAK-STAT cascade, TP53 and others in GO term “cell proliferation”, GO:0008283). Besides these, enrichment of proteins involved in cell motility (cytokines and cell adhesion molecules in GO term “cell locomotion”, GO:0040011) was detected, suggesting IL-1 $\alpha$ -dependent changes in cell morphology and migration. These results were consistent with observed alterations in HCT116 cell morphology (Fig. 3).

The enrichment in certain GO terms in the constructed PPI network suggests that interleukin-1 $\alpha$  could affect these pathways by transducing the signal through downstream cytokines. Consequently, we decided to experimentally investigate cell functions pointed out by the GO terms.

### 3.2. Exogenous IL-1 $\alpha$ -pretreated HCT116 and HCT116/FU cells are more sensitive to 5-FU

Enrichment in cell proliferation and cell death pathways was observed in the PPI network, therefore we assessed the sensitivity of the rhIL-1 $\alpha$ -pretreated cells to a cytotoxic drug 5-FU. For the experiments we used HCT116 cells and their 5-FU resistant subline HCT116/FU. As

we sought to induce at least comparable response of cells despite their chemoresistance status, a cytotoxic dose of 5-FU which results in reducing cell viability by 30 percent (CtD30) at 24 h after treatment was selected for both cell lines (see Section 2). In case the cytotoxicity differed from the preset value by more than 0.15, the results of the experiment were not taken into account. The treatment with both rhIL-1 $\alpha$  and IL-1Ra alone had no toxicity to the cells (Fig. 4a and b). However, it should be noted that treatment with rhIL-1 $\alpha$ , alone and in combination with 5-FU (further in text abbreviated as “IL-1 $\alpha$  + FU”), had a significant impact on cell morphology (Fig. 3). We observed clear differences compared to the control cells already after 48 h post-seeding, which is the time point we chose for treating cells with chemotherapeutic drugs.

Combined IL-1 $\alpha$  + FU treatment had a significant effect on HCT116 cells (Fig. 4a) ( $p < 0.001$  and Cohen’s  $d = 2.74$ , in comparison with 5-FU alone) but not on HCT116/FU cells (Fig. 4b) at 24 h after treatment. On the other hand, at 48 h post-treatment, IL-1 $\alpha$  + FU significantly reduced cell viability, in comparison with 5-FU alone, in both cell lines ( $p < 0.001$ ,  $d = 3.20$  for HCT116 cells and  $p < 0.05$  with  $d = 4.00$  for HCT116/FU cells). In order to exclude the possibility that the results of the crystal violet-based assays were due to the changes in cell morphology and not because of an actual loss of viability, we also performed cell counting (data not shown), and the results were in accordance with the data shown in Fig. 4a and b.

### 3.3. Endogenous IL-1 $\alpha$ positively impacts cell sensitivity to 5-FU in HCT116 cells but not in HCT116/FU cells

Our next question was addressed to intracellular IL-1 $\alpha$  activity, as exogenous IL-1 $\alpha$  significantly increased the expression of *IL1A* gene in both HCT116 and HCT116/FU cells (Fig. 4c). For this reason we performed siRNA-based silencing of the *IL1A* gene in HCT116 and HCT116/FU cells, followed by cytotoxic treatment with 5-FU. As HCT116/FU cells were not chemoresistant to a chemotherapeutic drug oxaliplatin (OxaPt) (as characterized in [7]), OxaPt was used as a positive control.

We detected (Fig. 4d) that silencing of *IL1A* significantly increases the sensitivity of HCT116 cells to 5-FU treatment (further referred to as si*IL1A* + FU) at 48 h post-treatment ( $p = 0.011$ , siNT + FU vs. si*IL1A* + FU). As distinct from 5-FU, the effect of OxaPt treatment was significantly increased in si*IL1A*-transfected (si*IL1A* + OxaPt) cells in both HCT116 ( $p < 0.001$ , siNT + OxaPt vs. si*IL1A* + OxaPt) and HCT116/FU ( $p = 0.004$ , siNT + OxaPt vs. si*IL1A* + OxaPt) cells. We conclude that, with respect to chemoresistance to 5-FU cytotoxicity, endogenous *IL1A* has significant impact only on the chemosensitive (HCT116) cells.

### 3.4. Exogenous IL-1 $\alpha$ alters 5-FU-induced cell death but not cell cycle arrest

The cytotoxic effect of 5-FU to living cells is based on the damage to the nucleic acids, eventually inducing either cell cycle arrest or cell death. Therefore, next we wanted to understand which cellular mechanisms are responsible for the reduction in viability we observed. The cell cycle investigation was performed by flow cytometry.

The cell cycle analysis (Fig. 5a and b) has not shown any significant differences in distribution of cells throughout the cell cycle phases, comparing either control cells vs. ones, treated with exogenous IL-1 $\alpha$  or IL-1Ra alone. The same was observed, comparing 5-FU-treated cells vs. treated with combinations of 5-FU and recombinant proteins. However, it should be noted that 24 h post-treatment with 5-FU alone (CtD30), only HCT116 cells induced cell cycle arrest (Fig. 5a); and after 48 h of treatment, cell cycle arrest of a similar fashion was observed in both HCT116 and HCT116/FU cells (Fig. 5b), suggesting a delayed response of HCT116/FU cells in terms of cell cycle arrest to cytotoxic 5-FU treatment. On the other hand, data analysis suggested a significant subpopulation of sub-G1 cells (see Section 2) being detected in the

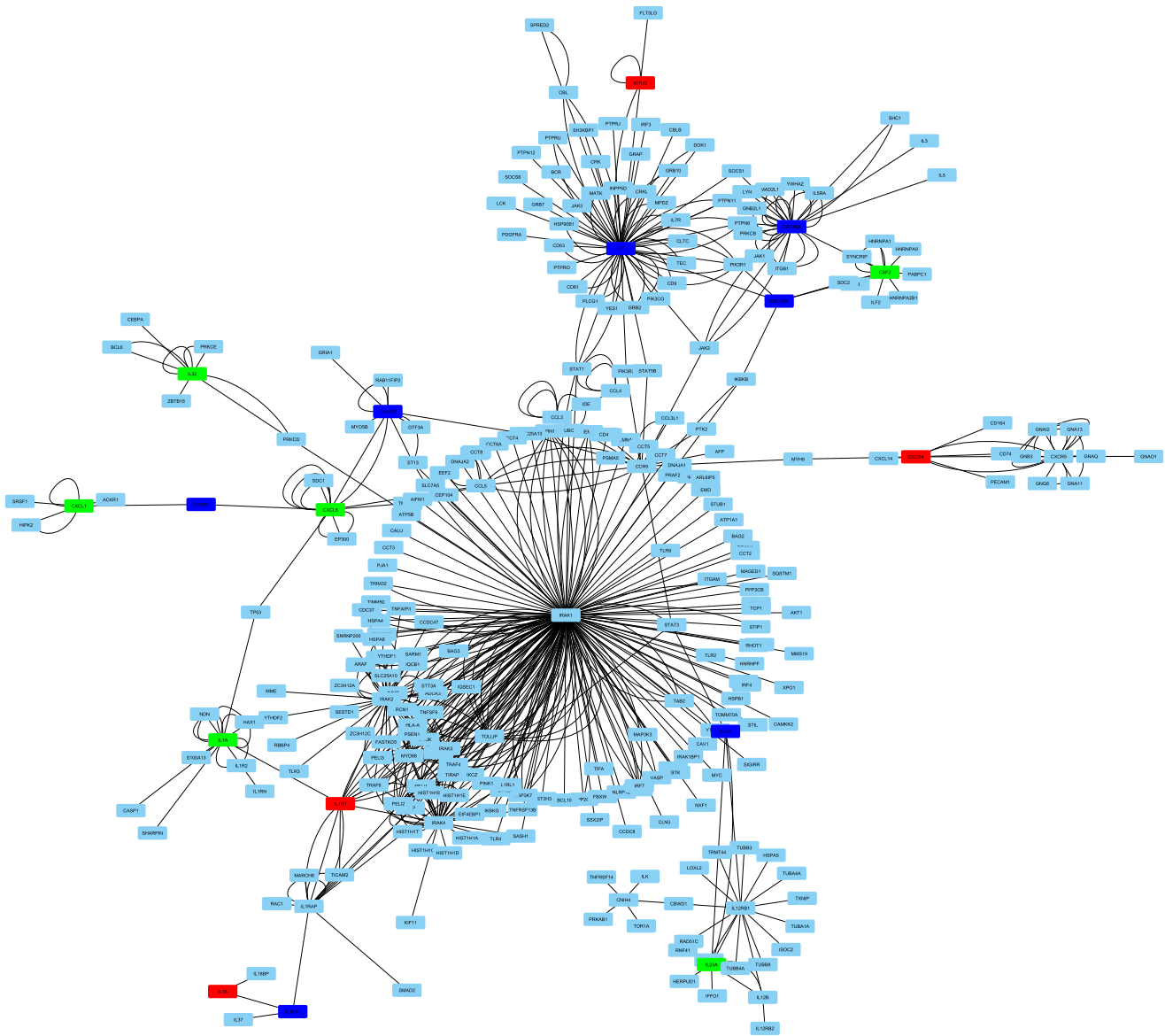


**Fig. 2.** Protein-protein interaction network, based on cytokines which are upregulated or downregulated upon increased exogenous IL-1 $\alpha$  signaling. Cytokines and their respective receptors from Table 2 were used as the seed nodes for building this protein-protein interaction network. Green color, cytokines which gene expression was upregulated (*IL1A, IL32, CSF2, CXCL8, IL23A, CXCL1*) upon treatment with rhIL-1 $\alpha$ ; red color, downregulated cytokines (*IL11, CXCR4, IL18, KITLG, IL1R1*); blue color, respective receptors of these cytokines (*CSF2RA, CSF2RB, CXCR1, CXCR2, IL23R, IL18RB, KIT*). (For interpretation of the references to color in this figure legend, the reader is referred to the web version of this article.)

**Table 3**

Selected results of Gene Ontology analysis of the protein-protein interaction network, using *PATHER GO-Slim Biological Process* set of GO terms. Marked with “\*” are GO terms, which included IL-1 $\alpha$ . Arrows on the Column #2 mark either activating (↑) or inhibitory (↓) effect on the pathway of the proteins, present in the PPI network.

GO term	Effect of PPI network proteins	Enrichment of the network, folds	p-value
Regulation of sequence-specific DNA binding transcription factor activity (GO:0051090)	↑	19.99	$2.14 \times 10^{-5}$
Cytokine-mediated signaling pathway (GO:0019221)*	↑	9.79	$5.07 \times 10^{-9}$
Localization (GO:0051179)	↑	9.47	$1.81 \times 10^{-9}$
Cell proliferation (GO:0008283)*	↓	9.04	$2.30 \times 10^{-10}$
JAK-STAT cascade (GO:0007259)	↑/↓	8.69	$3.29 \times 10^{-4}$
Locomotion (GO:0040011)*	↑	7.91	$7.98 \times 10^{-9}$
I- $\kappa$ B kinase/NF- $\kappa$ B cascade (GO:0007249)*	↑	6.66	$2.58 \times 10^{-2}$
Cell differentiation (GO:0030154)*	↑/↓	6.45	$2.68 \times 10^{-2}$

treatments involving 5-FU treatment after 48 h (Fig. S3). Therefore, an excessive amount of cell population having its DNA being degraded at that time point suggested us to perform a cell death mode assay.

Thus, further on, we studied the cell death modes upon combined treatment of cells with 5-FU and recombinant proteins, using fluorescence microscopy. Since we collected both the cells attached to the

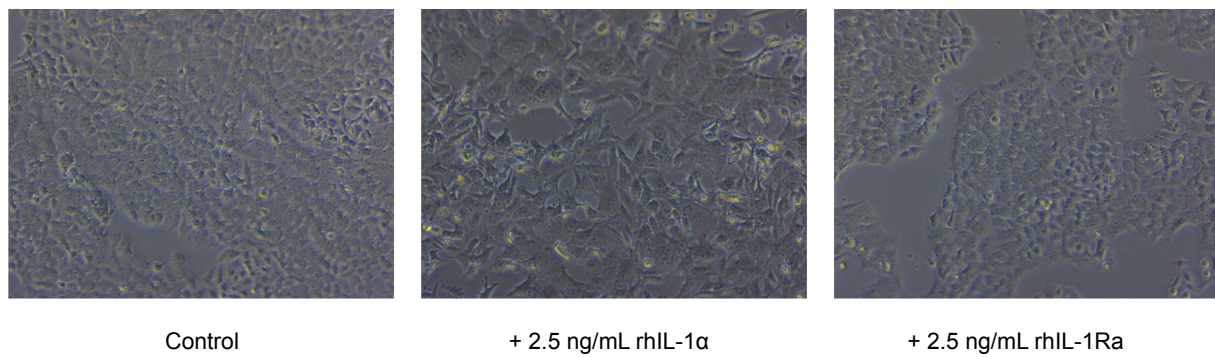


**Fig. 3.** Changes in the morphology of HCT116 cells upon 48 h treatment with recombinant IL-1α (center) or IL-1Ra (right), compared with control (left). Cells were seeded to culture dishes and cell cultivation medium was supplemented with recombinant IL-1α or IL-1Ra to the final concentration of 2.5 ng/mL of cell cultivation medium just after seeding and incubated for 48 h and pictures were captured with a bright-field light microscope. Control, no treatment with recombinant proteins.

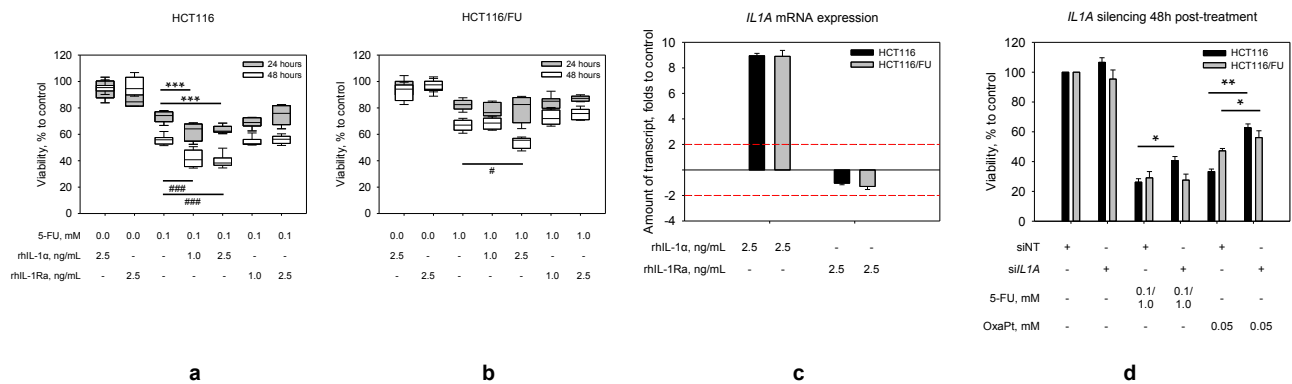


**Fig. 4.** The impact of combined treatment of 5-FU and recombinant IL-1α or IL-1Ra to the sensitivity of HCT116 and HCT116/FU cells to 5-FU-induced cytotoxic treatment 24 h (a) or 48 h (b) after induction of cytotoxic effect. a Cells were seeded to culture dishes and cell cultivation medium was supplemented with recombinant IL-1α or IL-1Ra just after seeding. Then cells were treated with 0.1 mM (HCT116) or 1.0 mM (HCT116/FU) of 5-FU at 48 h after seeding. 24 h after the induction of cytotoxic effect, cells were fixed and subjected to crystal violet staining. b Cells were seeded and treated with 5-FU as in (a). 24 h after the induction of cytotoxic effect, cell culture medium was changed and supplemented with the same amount with recombinant proteins as immediately after seeding (see Section 2). Additional 24 h after, cells were fixed and subjected to crystal violet staining. Control, no treatment with recombinant proteins and 5-FU. \* marks level of significance in 24 h post-treatment, # - in 48 h post-treatment. RM ANOVA was performed for evaluation of rhIL-1α, alone and in combination, effect significance, which could not be sense by averaging the data of biological replicates. Error bars, ± SD.

The impact of recombinant IL-1α to the expression of *IL1A* in HCT116 and HCT116/FU cells (c) and silencing of *IL1A* to sensitivity to 5-FU or OxaPt-induced cytotoxic treatment after 48 h (d). c Cells were seeded and incubated with 2.5 ng/mL of recombinant proteins for 96 h, then collected and subjected to RNA extraction, followed by cDNA synthesis and qPCR. Normalization was performed, using *B2M* as a house-keeping gene. Control, no treatment with recombinant proteins and 5-FU. Error bars, ± SD. d Cells were transfected with either non-targeting (siNT) or human *IL1A*-specific (si*IL1A*) siRNA at 24 h after cell seeding. 48 h post-seeding, cytotoxic effect was induced by using 0.1/1.0 mM of 5-FU (for HCT116 and HCT116/FU cells, respectively) or 0.05 mM of OxaPt (for both cell lines). 24 h after induction, cell cultivation medium was changed, then cells were fixed and subjected to crystal violet staining 48 h after induction of cytotoxic effect. Control, transfection with siNT and no cytotoxic treatment. Error bars, ± SD. (For interpretation of the references to color in this figure legend, the reader is referred to the web version of this article.)

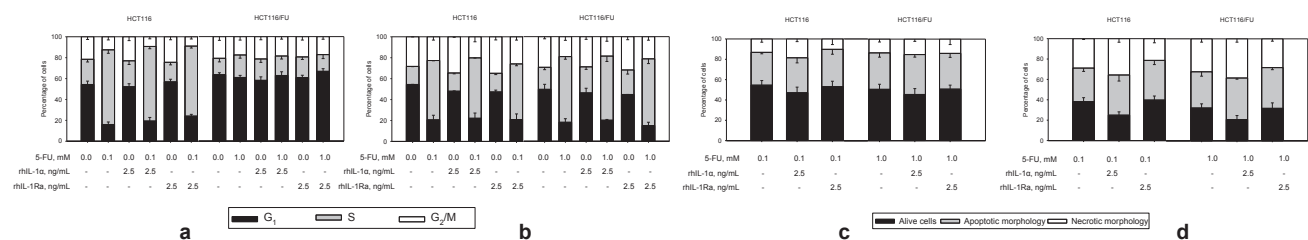


**Fig. 5.** The impact of combining 5-FU and recombinant IL-1R ligands to cytotoxic treatment-induced cell cycle arrest (a and b) and cell death mode (c and d) 24 or 48 h post-treatment in HCT116 and HCT116/FU cells. a, b Cells were treated with 0.1 mM (HCT116) or 1.0 mM (HCT116/FU) of 5-FU at 48 h after cell seeding. For (a), 24 h after the induction of cytotoxic effect (CtD30), cells were collected and analyzed by flow cytometry. For (b), 24 h after the induction of cytotoxic effect, cell culture medium was changed and supplemented with the same amount with recombinant proteins as immediately after seeding. Additional 24 h after (CtD50), cells were collected and analyzed by flow cytometry. c, d Cells were treated with 0.1 mM (HCT116) or 1.0 mM (HCT116/FU) of 5-FU at 48 h after cell seeding. For (c), 24 h after the induction of cytotoxic effect (CtD30), cells and cell culture medium were collected and cells were analyzed by fluorescence microscopy. For (d), 24 h after the induction of cytotoxic effect, cell culture medium was changed and supplemented with the same amount with recombinant proteins as immediately after seeding. Additional 24 h after (CtD50), cells and cell culture medium were collected and cells were analyzed by fluorescence microscopy. Control, no treatment with recombinant proteins and 5-FU; CtD, cytotoxic dose. Error bars, ± SD.

**Table 4**

Results of cell death mode assays at 48 h after treatment and analysis of Holm-Šídák post-hoc statistical tests. Fractions of each cell morphology type are provided as mean ± SD.

Cell line	HCT116			HCT116/FU			
	Treatment	FU	IL + FU	Ra + FU	FU	IL + FU	Ra + FU
Alive cells, %		38.2 ± 3.9	25.0 ± 3.2	39.8 ± 3.9	32.1 ± 4.1	20.8 ± 3.9	31.8 ± 5.3
Apoptotic morphology, %		32.9 ± 3.2	39.4 ± 6.0	38.9 ± 4.1	35.6 ± 4.3	40.8 ± 1.1	39.9 ± 2.0
Necrotic morphology, %		28.9 ± 0.8	36.7 ± 3.5	21.3 ± 4.0	32.3 ± 3.3	38.4 ± 3.3	28.2 ± 2.3
Treatments tested		FU vs IL + FU	FU vs Ra + FU	IL + FU vs Ra + FU	FU vs IL + FU	FU vs Ra + FU	IL + FU vs Ra + FU
Alive cells		<b>p &lt; 0.01</b>	n.s.	<b>p &lt; 0.01</b>	<b>p &lt; 0.001</b>	n.s.	<b>p &lt; 0.001</b>
Apoptotic morphology		n.s.	n.s.	n.s.	<b>p = 0.001</b>	n.s.	<b>p = 0.001</b>
Necrotic morphology		<b>p &lt; 0.01</b>	<b>p = 0.01</b>	<b>p &lt; 0.001</b>	<b>p &lt; 0.001</b>	<b>p &lt; 0.01</b>	<b>p &lt; 0.05</b>

Abbreviations: n.s., not significant; FU, treatment with 5-FU alone; IL + FU, combination treatment with 5-FU and rhIL-1α; Ra + FU, combination treatment with 5-FU and rhIL-1Ra. Statistical significance between the groups compared (p < 0.05) is marked in bold.

surface of culture dishes and cell culture medium, we observed a basal level of cells, undergoing cell death with apoptotic (16.8 ± 2.4%) and necrotic (6.7 ± 1.1%) cell morphology in control samples in both cell lines at 24 and 48 h after treatment. As it can be seen in Fig. 5c, no significant differences in cell death were observed 24 h post-treatment in both HCT116 and HCT116/FU cell lines, comparing 5-FU treated cells vs. cells treated with IL-1α + FU. However, at 48 h post-treatment (detailed results of the post-hoc tests provided in Table 4), we registered significant differences in intensity of cell death (Fig. 5d): for HCT116 cells, a significant increase of cells, possessing necrotic morphology (IL-1α + FU vs. FU; p = 0.001) was detected. As for HCT116/FU cells, IL-1α + FU led to an increase of cells, showing both apoptosis- (IL-1α + FU vs. 5-FU, p = 0.001) and necrosis-like (IL-1α + FU vs. FU; p = 0.026) morphological signatures. Our data suggests that treatment with exogenous IL-1α significantly promotes 5-FU-induced necrosis-like cell death in HCT116 cells or both apoptosis- and necrosis-like cell death in HCT116/FU cells.

**3.5. Treatment with both 5-FU and exogenous IL-1α alters gene expression of cell adhesion molecules**

In accordance with the enrichment of the proteins, responsible for cell locomotion in our PPI network (Table 3), we noticed that treatment of both cell lines with recombinant proteins causes alterations in cell morphology (Fig. 3). In the light of results described above, we sought to address the effects of exogenous IL-1α and 5-FU on the gene expression of cell adhesion molecules having an established clinical role in cancer (according to [17]: CDH1 (E-cadherin), CDH2 (N-cadherin), CTNNB1 (β-catenin), CLDN2 (claudin-2), SELE (E-selectin), ITGB6 (integrin β6) and VCL (vinculin). The results of the qPCR assays are shown in Table 5 and in Supplementary Fig. S4.

For E-cadherin, both 5-FU and rhIL-1α, alone and in combination, downregulated the expression of CDH1 in both chemosensitive and chemoresistant cell lines after 24 h post-treatment, and effect sizes for

**Table 5**

Results of mRNA expression assays of selected cell adhesion molecules. Symbols: fc ≥ 2 upregulation of the gene expression (↑), downregulation (↓) or no significant change in gene expression detected (–).

Cell line	Treatment	CDH1	CDH2	SELE	CLDN2	ITGB6
HCT116	5-FU	↓	↓	↑	↓	–
	rhIL-1α	↓	↓	–	–	↓
	5-FU + rhIL-1α	↓	–	↑	↓	↑
	rhIL-1Ra	–	–	–	–	–
	5-FU + rhIL-1Ra	–	–	↑	–	↑
HCT116/FU	5-FU	↓	–	–	↓	–
	rhIL-1α	↓	↓	–	–	↓
	5-FU + rhIL-1α	↓	–	↑	↓	↓
	rhIL-1Ra	–	–	–	–	–
	5-FU + rhIL-1Ra	–	–	–	–	–

all the treatments were similar. As for N-cadherin, it was evaluated that CDH2 expression in untreated HCT116/FU cells was up to 70 times lower, compared to untreated HCT116 cells. Furthermore, significant downregulation of CDH2 up to 24 times was detected in HCT116 cells upon treatment either with 5-FU or rhIL-1α, but not upon IL-1α + FU treatment. In chemoresistant cells, the tangible downregulation of CDH2 up to three times was observed only when the cells were treated with recombinant IL-1α. The expression of β-catenin gene CTNNB1, coding an adapter protein for cadherins, was not changing significantly in any kind of treatments in both cell lines (data not shown).

SELE (coding E-selectin) was found to be significantly upregulated up to four times in HCT116 cells, treated with 5-FU, alone and in a combinations of either rhIL-1α or rhIL-1Ra, while in HCT116/FU cells only IL-1α + FU yielded about 2.6 times more transcript, compared to control cells (Fig. S2c and d). Interestingly, in response to 5-FU, CLDN2 (Claudin-2) was downregulated in both cell lines up to three times, and cell response to IL-1α + FU was more profound, as expression of CLDN2 was decreased up to eight times.

ITGB6 gene, coding integrin β6, was observed to be downregulated upon treatment with rhIL-1α alone in both cell lines. Unlike rhIL-1α, effect of IL-1α + FU downregulated ITGB6 up to four times in HCT116 cells and upregulated the gene up to three times in HCT116/FU cells. The expression of VCL, coding adapter protein for integrins, was not changing significantly after any kind of treatments in both cell lines (data not shown).

**4. Discussion**

After screening of mRNA expression patterns of selected cytokines in HCT116 cells stimulated with exogenous IL-1α (Figs. S1 and S2, Table 2), first we constructed and functionally annotated a protein-protein interaction network that contains cytokines which showed altered expression after 96 h of stimulus, their receptors and all the proteins interacting with them (Fig. 2, Table 3). Enrichment of proteins participating in pathways associated with cell survival and death was observed in this network. Therefore we started our experimental study by addressing the effects of IL-1α to the response of both parental HCT116 and chemoresistant HCT116/FU cells to the treatment with a cytotoxic chemotherapeutic drug 5-FU. In HCT116 cells, both exogenous and endogenous IL-1α significantly increased cell sensitivity to 5-FU (Fig. 4a and d). In HCT116/FU cells, only exogenous IL-1α had positive effect on cell sensitivity to 5-FU (Fig. 4b and d). This suggests downregulation of endogenous IL-1α signaling in HCT116/FU cells, and involvement of the IL-1α signaling pathway in cell death.

There is a number of studies with controversial results that assign a pro- or anti-proliferative function to IL-1α, depending on the cell model, used in the study [18–21]. However, endogenous IL-1α was shown to be recruited to the sites of DNA damage, where it might act as a DNA damage sensor [22]. As 5-FU treatment is known to induce the DNA damage response and subsequently cell cycle arrest and cell death

[23], the downregulation of endogenous IL-1 $\alpha$  signaling might be the one of several ways to reduce the HCT116/FU cell sensitivity to the DNA damage and to evade the cell death. It should be noted, however, that recent experimental evidence, showing sensitization to EGFR inhibitor erlotinib of previously erlotinib-resistant head and neck squamous cell carcinoma cells upon IL-1R blockade with IL-1Ra [24], suggests that the cellular effects, mediated through IL-1R signal transduction pathway might be fine-tuned in a context-dependent manner.

On the other hand, the exogenous IL-1 $\alpha$  in combination with 5-FU significantly increased cell death with apoptotic morphology in both cell lines. It is consistent with other studies on significance of exogenous IL-1 $\alpha$  in osteoblast cells for the induction of apoptosis [25]. An important point is that the effect of IL-1 $\alpha$  + FU determined a higher level of cells possessing necrotic morphology than a single effect of 5-FU, whereas the single IL-1 $\alpha$  did not have any significant effect on cell viability. Moreover, the effect of IL-1 $\alpha$  + FU significantly increased necrotic morphological signatures only in HCT116 cells, while in the HCT116/FU cells, necrosis-like cell death was delayed indicating a perturbation of the exogenous IL-1 $\alpha$  pathway that might allegedly lead to downregulation of the immune response in the chemoresistant cell line if transferred to an *in vivo* model system.

Loss of the plasma membrane integrity usually causes entering of the cell contents to the environment and inflammation. In this context, it is well documented that passive release of IL-1 $\alpha$  into extracellular matrix activates IL-1 receptors in neighboring cells. This causes an increase of IL-1 $\alpha$  biosynthesis, its exposure on the plasma membrane and/or passive release, resulting in a loop started by the initial IL-1 $\alpha$ -IL-1R binding [5]. Thus, according to the classical scheme, if 5-FU effect causes cell necrosis, then the IL-1 $\alpha$  protein leaves from the inside of the cell and enhances the effect of the single 5-FU in a similar fashion to that of combined effect IL-1 $\alpha$  + FU. We have indeed observed such a pattern of IL-1 $\alpha$  action in A-431 cells [26]. The fact, that in our study the effect of IL-1 $\alpha$  + FU is more pronounced than effect of single 5-FU treatment, does not contradict with the classical scheme, as IL-1 $\alpha$  is retained in HCT116 cells after cytotoxic treatments and is not recorded in the incubation medium of HCT116 cells [27]. Our results indicate that the cell survival response might be regulated by modulating the activity of exogenous form of the dual-action cytokine, especially, if the endogenous form the cytokine is retained inside the cell.

Indeed, we observed an enrichment of our PPI network with proteins participating in the processes, related to stress signaling and cell death, such as NF- $\kappa$ B signaling (GO:0007249). Usually NF- $\kappa$ B pathway activity is considered to be anti-apoptotic. However, there is some evidence suggesting a pro-apoptotic activity of NF- $\kappa$ B in cells, possessing active tumor suppressors (such as TP53 or p21) through increased expression of several pro-apoptotic genes [28]. As we used TP53-proficient HCT116 cells in our study, we postulate that alterations in NF- $\kappa$ B signaling might have a role in the increase of cell death we observed. On the other hand, an enrichment in JAK/STAT (GO:0007259) cascade proteins and proteins, associated with negative effects to cell differentiation (GO:0030154) was detected. Dedifferentiation of cells in general, as well as upregulated JAK/STAT signaling, is thought to mediate cell survival upon various types of tissue stress [29]. Thus, we hypothesize that these two axes might have an antagonistic relationship in the control of cell survival upon 5-FU-mediated cytotoxic treatment.

Another part of the study was the analysis of expression patterns of cell adhesion molecules at mRNA level, which has arisen from the analysis of annotated PPI network and our observations at the cell morphology level (Fig. 3). We have shown (Table 5, Fig. S4a and b) that expression of *CDH1* was downregulated in both cell lines treated with 5-FU, rhIL-1 $\alpha$  or a combination of them, while similar trend for *CDH2* was observed only in treatments with rhIL-1 $\alpha$  alone. Combination of downregulation of *CDH1* and upregulation of *CDH2* expression (also known as “cadherin switch”) is usually recognized as a major pair of

markers for epithelial-mesenchymal transition (EMT) [30]. Contrary to that, in our study we observed downregulations of both *CDH1* and *CDH2*: in a certain type of tumor model, it was shown that downregulation of *CDH2* has a negative impact to cell viability [31]. Interestingly, we detected a multiple-fold lesser expression (see Section 3.5) of *CDH2* in untreated HCT116/FU cells, compared to untreated HCT116 cells. Those observations suggest that in our cell system, chemoresistance of the cells could be regulated by modulation of N-cadherin expression.

Along with cadherins, alterations in expression of other cell adhesion molecules were observed (Fig. S4c and d). The expression of *SELE* was significantly upregulated in both HCT116 and HCT116/FU cells, treated with 5-FU, being even more profound upon IL-1 $\alpha$  + FU treatment. The upregulation of this gene was shown to be associated with increase of metastatic potential in CRC cell models *in vitro* [32] as well as upregulation of CXCL1, IL-6 and CXCL8 cytokines [33]. Therefore, these findings suggest an exogenous IL-1 $\alpha$ -dependent increase in metastatic potential in both HCT116 and HCT116/FU cells. Besides, we observed an increased expression of *CXCL1* and *CXCL8* gene expression (Fig. S1, Table 2) upon treatment of HCT116 cells with rhIL-1 $\alpha$ , which is in agreement with IL-1 $\alpha$ -dependent increase in secretion of CXCL8 protein, discussed in our previous report [27].

Significant downregulation of *CLDN2* gene was observed following IL-1 $\alpha$  + FU treatment as well, which was shown to be associated with increased metastatic potential and advanced disease in breast cancer models [34]. On the other hand, upregulation of *CLDN2* was recently reported to be associated with colorectal cancer cell stemness, which, in regard, is thought to be tightly linked to the increased chemoresistance of the cells [35]. This is indeed in accordance with our observation that treatment of the cells with 5-FU had a significant impact on *CLDN2* downregulation, while rhIL-1 $\alpha$  treatment had none.

Interestingly, *ITGB6* was found to be upregulated in HCT116 but downregulated in HCT116/FU cells upon IL-1 $\alpha$  + FU treatment. Expression of *ITGB6* was reported to be needed for metastasis of colorectal cancer cells [36], and for proliferation signaling through FAK/STAT3 axis [37]. Thus, we speculate that *ITGB6* gene expression might be controlled by both cell proliferation and migration pathways and is a subject to an equilibrium-like relationship between upregulating stimuli (exogenous IL-1 $\alpha$  signaling) and downregulating ones (cytotoxic effect-induced cell death).

Besides the enrichment in cell adhesion molecules in our PPI network, we detected that the exogenous IL-1 $\alpha$ -induced increase in the metastatic potential of the cells (locomotion, GO:0040011) might be dependent on rearrangement of extracellular matrix (ECM) as well. For instance, IL-1 $\alpha$  signaling is known to induce the expression of matrix metalloproteinase 7 (MMP7), which enables cell metastasis through shedding of ECM components [38]. Along the upregulated breakdown of ECM components, the increase in expression of ECM proteoglycans syndecan-1 and -2 is detected, which are thought to be important as coreceptors for chemokines and growth factors. Cytokine-induced JAK/STAT and NF- $\kappa$ B signaling (upregulation of which was also a prominent feature of our PPI network) is thought to be important for the control of the expression of these [39].

To sum up, our results lead towards two major conclusions: that upregulated exogenous IL-1 $\alpha$  signaling results in (a) higher chemosensitivity and (b) altered cell adhesion molecule expression pattern, which, according to data present, could be associated with an increase of the metastatic potential in our model; the latter being extremely important in clinical treatment of phase III-IV tumors. Monotherapy with an IL-1 $\alpha$ -targeting human antibody has successfully passed the Phase I clinical trial [40], yet Phase III study was terminated in June 2017 (ClinicalTrials.gov ID NCT01767857). Recombinant human IL-1Ra, also known as Anakinra, is currently in the clinical trials as a combined therapy for many inflammation-associated diseases, including cancer [41]: Phase II clinical trial on combination of Anakinra with chemotherapeutics for metastatic CRC was finished in May 2017

(NCT02090101). Another recent report [42], including both in vivo experiments and a pilot clinical study, has identified IL-1Ra-dependent transcriptional signature and stratified prospective clinical uses of IL-1R-targeted therapy in treatment of metastatic breast cancers. As advanced cancer cases are characterized by their metastatic nature and are highly dependent on the proinflammatory tumor microenvironment, our data support the prospects of using strategies, targeting exogenous IL-1 $\alpha$  signaling, in the treatment of advanced and chemoresistant tumors.

## Acknowledgments

This work has been supported by the Research Council of Lithuania, grants SEN-17/2015 and SMT15P-070.

## Competing interests

The authors declare no competing interests present.

## Appendix A. Supplementary material

Supplementary data to this article can be found online at <https://doi.org/10.1016/j.cyto.2018.11.031>.

## References

- Mercedes Navarro, et al., Colorectal cancer population screening programs worldwide in 2016: an update, *World J. Gastroenterol.* 23 (20) (2017) 3632, <https://doi.org/10.3748/wjg.v23.i20.3632>.
- Minoru Koi, John M. Carethers, The colorectal cancer immune microenvironment and approach to immunotherapies, *Future Oncol.* 13 (18) (2017) 1633–1647, <https://doi.org/10.2217/fon-2017-0145>.
- Qian Liu, et al., The CXCL8-CXCR1/2 pathways in cancer, *Cytok. Growth Factor Rev.* 31 (Oct.) (2016) 61–71, <https://doi.org/10.1016/j.cytogfr.2016.08.002>.
- Valerio Gelfo, et al., A module of inflammatory cytokines defines resistance of colorectal cancer to EGFR inhibitors, *Oncotarget* 7 (44) (2016), <https://doi.org/10.18632/oncotarget.12354>.
- Nelson C. Di Paolo, Dmitry M. Shayakhmetov, Interleukin 1 $\alpha$  and the inflammatory process, *Nat. Immunol.* 17 (8) (2016) 906–913, <https://doi.org/10.1038/ni.3503>.
- Anna Acheva, et al., Pro-Inflammatory signaling in a 3D organotypic skin model after low LET irradiation—NF- $\kappa$ B, COX-2 activation, and impact on cell differentiation, *Front. Immunol.* 8 (Feb.) (2017), <https://doi.org/10.3389/fimmu.2017.00082>.
- Egle Kukcinaviciute, et al., Significance of Notch and Wnt signaling for chemoresistance of colorectal cancer cells HCT116, *J. Cell. Biochem.* 119 (7) (2018) 5913–5920, <https://doi.org/10.1002/jcb.26783>.
- Donald Wlodkowic, et al., Flow cytometry-based apoptosis detection, *Methods in Molecular Biology*, Humana Press, 2009, pp. 19–32 [https://doi.org/10.1007/978-1-60327-017-5\\_2](https://doi.org/10.1007/978-1-60327-017-5_2).
- Sandra Orchard, et al., The MIntAct project—IntAct as a common curation platform for 11 molecular interaction databases, *Nucl. Acids Res.* 42 (D1) (2013) D358–D363, <https://doi.org/10.1093/nar/gkt115>.
- Andrew Chatr-Aryamontri, et al., The BioGRID interaction database: 2017 update, *Nucl. Acids Res.* 45 (D1) (2016) D369–D379, <https://doi.org/10.1093/nar/gkw1102>.
- P. Shannon, Cytoscape: a software environment for integrated models of biomolecular interaction networks, *Genome Res.* 13 (11) (2003) 2498–2504, <https://doi.org/10.1101/gr.1239303>.
- Michael Ashburner, et al., Gene ontology: tool for the unification of biology, *Nat. Genet.* 25 (1) (2000) 25–29, <https://doi.org/10.1038/75556>.
- The Gene Ontology Consortium, Expansion of the gene ontology knowledgebase and resources, *Nucl. Acids Res.* 45 (D1) (2017) D331–D338, <https://doi.org/10.1093/nar/gkw1108>.
- Huayui Mi, Xiaosong Huang, Anushya Muruganujan, Haiming Tang, Caitlin Mills, Diane Kang, Paul D. Thomas, PANTHER version 11: expanded annotation data from Gene Ontology and Reactome pathways, and data analysis tool enhancements, *Nucl. Acids Res.* 45 (D1) (2017) D183–D189, <https://doi.org/10.1093/nar/gkw1138>.
- Gail M. Sullivan, Richard Feinn, Using effect size—or why the P value is not enough, *J. Grad. Med. Edu.* 4 (3) (2012) 279–282, <https://doi.org/10.4300/jgme-d-12-00156.1>.
- A.V. Orjalo, et al., Cell surface-bound IL-1 $\alpha$  is an upstream regulator of the senescence-associated IL-6/IL-8 cytokine network, *Proc. Natl. Acad. Sci.* 106 (40) (2009) 17031–17036, <https://doi.org/10.1073/pnas.0905299106>.
- Nektaria Makrilia, et al., Cell adhesion molecules: role and clinical significance in cancer, *Canc. Investig.* 27 (10) (2009) 1023–1037, <https://doi.org/10.3109/07357900902769749>.
- J.A. Maier, et al., Extension of the life-span of human endothelial cells by an interleukin-1 alpha antisense oligomer, *Science* 249 (4976) (1990) 1570–1574.
- J.S. Wolf, et al., IL (interleukin)-1alpha promotes nuclear factor-kappaB and AP-1-induced IL-8 expression, cell survival, and proliferation in head and neck squamous cell carcinomas, *Clin. Canc. Res.* 7 (6) (2001) 1812–1820.
- S.L. Maund, et al., Interleukin-1 $\alpha$  mediates the antiproliferative effects of 1,25-dihydroxyvitamin D3 in prostate progenitor/stem cells, *Cancer Res.* 71 (15) (2011) 5276–5286, <https://doi.org/10.1158/0008-5472.can-10-2160>.
- Jung Yoon Bae, et al., Reciprocal interaction between carcinoma-associated fibroblasts and squamous carcinoma cells through interleukin-1 $\alpha$  induces cancer progression, *Neoplasia* 16 (11) (2014) 928–938, <https://doi.org/10.1016/j.neo.2014.09.003>.
- Idan Cohen, et al., IL-1 $\alpha$  is a DNA damage sensor linking genotoxic stress signaling to sterile inflammation and innate immunity, *Sci. Rep.* 5 (Oct.) (2015) 14756, <https://doi.org/10.1038/srep14756>.
- B.L. Adamsen, K.L. Kravik, P.M. De Angelis, DNA damage signaling in response to 5-fluorouracil in three colorectal cancer cell lines with different mismatch repair and TP53 status, *Int. J. Oncol.* 39 (3) (2011) 673–682.
- Aditya Stanam, et al., Interleukin-1 blockade overcomes erlotinib resistance in head and neck squamous cell carcinoma, *Oncotarget* 7 (46) (2016), <https://doi.org/10.18632/oncotarget.12590>.
- Chun Guo, et al., IL-1 $\alpha$  induces apoptosis and inhibits the osteoblast differentiation of MC3T3-E1 Cells through the JNK and p38 MAPK pathways, *Int. J. Mol. Med.* 38 (1) (2016) 319–327, <https://doi.org/10.3892/ijmm.2016.2606>.
- Daiva Dabkeviciene, et al., Differential expression of VEGF and IL-1alpha after photodynamic treatment in combination with doxorubicin or taxotere, *Antica. Res.* 34 (10) (2014) 5295–5302.
- Daiva Dabkeviciene, et al., The role of interleukin-8 (CXCL8) and CXCR2 in acquired chemoresistance of human colorectal carcinoma Cells HCT116, *Med. Oncol.* 32 (12) (2015), <https://doi.org/10.1007/s12032-015-0703-y>.
- Sonia Rocha, et al., Regulation of NF- $\kappa$ B and p53 through activation of ATR and Chk1 by the ARF tumour suppressor, *EMBO J.* 24 (6) (2005) 1157–1169, <https://doi.org/10.1038/sj.emboj.7600608>.
- Marco La Fortezza, et al., JAK/STAT signalling mediates cell survival in response to tissue stress, *Development* 143 (16) (2016) 2907–2919, <https://doi.org/10.1242/dev.132340>.
- Min Wang, et al., N-cadherin promotes epithelial-mesenchymal transition and cancer stem cell-like traits via ErbB signaling in prostate cancer cells, *Int. J. Oncol.* 48 (2) (2015) 595–606, <https://doi.org/10.3892/ijo.2015.3270>.
- Felix Bremmer, et al., Role of N-cadherin in proliferation, migration, and invasion of germ cell tumours, *Oncotarget* 6 (32) (2015), <https://doi.org/10.18632/oncotarget.5288>.
- Tegest Aycheh, et al., E-selectin regulates gene expression in metastatic colorectal carcinoma cells and enhances HMGB1 release, *Int. J. Cancer* 123 (8) (2008) 1741–1750, <https://doi.org/10.1002/ijc.23375>.
- Pu Zhang, et al., Melanoma upregulates ICAM-1 expression on endothelial cells through engagement of tumor CD44 with endothelial E-selectin and activation of a PKC $\alpha$ -p38-SP-1 pathway, *FASEB J.* 28 (11) (2014) 4591–4609, <https://doi.org/10.1096/fj.11-202747>.
- T.H. Kim, et al., Down-regulation of claudin-2 in breast carcinomas is associated with advanced disease, *Histopathology* 53 (1) (2008) 48–55, <https://doi.org/10.1111/j.1365-2559.2008.03052.x>.
- Sophie Paquet-Fifield, et al., Tight junction protein claudin-2 promotes self-renewal of human colorectal cancer stem-like cells, *Canc. Res.* 78 (11) (2018) 2925–2938, <https://doi.org/10.1158/0008-5472.can-17-1869>.
- Guang-Yun Yang, et al., Integrin alphavbeta6 mediates the potential for colon cancer cells to colonize in and metastasize to the liver, *Canc. Sci.* 99 (5) (2008) 879–887, <https://doi.org/10.1111/j.1349-7006.2008.00762.x>.
- Nishant P. Visavadiya, et al., Integrin-FAR signaling rapidly and potently promotes mitochondrial function through STAT3, *Cell Commun. Signal.* 14 (1) (2016), <https://doi.org/10.1186/s12964-016-0157-7>.
- Mi-Jung Kwon, et al., Interleukin-1 $\alpha$  promotes extracellular shedding of syndecan-2 via induction of matrix metalloproteinase-7 expression, *Biochem. Biophys. Res. Commun.* 446 (2) (2014) 487–492, <https://doi.org/10.1016/j.bbrc.2014.02.142>.
- Sherif Abdelaziz Ibrahim, et al., Syndecan-1 is a novel molecular marker for triple negative inflammatory breast cancer and modulates the cancer stem cell phenotype via the IL-6/STAT3, Notch and EGFR signaling pathways, *Mol. Canc.* 16 (1) (2017), <https://doi.org/10.1186/s12943-017-0621-z>.
- David S. Hong, et al., MABp1, a First-in-class true human antibody targeting interleukin-1 $\alpha$  in refractory cancers: an open-label, phase 1 dose-escalation and expansion study, *Lanc. Oncol.* 15 (6) (2014) 656–666, [https://doi.org/10.1016/s1470-2045\(14\)70155-x](https://doi.org/10.1016/s1470-2045(14)70155-x).
- Charles A. Dinarello, Why not treat human cancer with interleukin-1 blockade? *Canc. Metast. Rev.* 29 (2) (2010) 317–329, <https://doi.org/10.1007/s10555-010-9229-0>.
- Te-Chia Wu, et al., IL1 receptor antagonist controls transcriptional signature of inflammation in patients with metastatic breast cancer, *Canc. Res.* 78 (18) (2018) 5243–5258, <https://doi.org/10.1158/0008-5472.can-18-0413>.